Cdc42 reactivation at growth sites is regulated by cell-cycle-dependent removal of its GAP Rga4 in fission yeast

Julie Rich-Robinson, Afton Russell, Eleanor Mancini, Maitreyi Das*

Department of Biochemistry & Cellular and Molecular Biology, University of Tennessee, Knoxville, TN, USA, 37996.

*Corresponding author: mdas@utk.edu

Abstract

Cells undergo polarized growth to acquire shapes that promote function. In fission yeast, polarized cell growth is driven by the Morphogenesis Orb6 (MOR) pathway and the small GTPase Cdc42. After cell division, the MOR pathway first promotes cell separation, the final step in cytokinesis, and then promotes polarized growth at the cell ends. It is unclear how the ends initiate growth after the cells separate. It is plausible that the MOR pathway activates end growth only after successful cell separation. To test this, we developed a system whereby we delay cytokinesis, while mitosis progresses, via a temporary Latrunculin A (LatA) treatment. Mitotic cells treated with LatA, when allowed to recover, initiate end growth without cell separation. We call this the PrESS phenotype – polar elongation sans cell separation. PrESS cells reactivate Cdc42 at the ends before completing cytokinesis, indicating that these are independent processes. Cell ends siphon away Cdc42, its regulators, and trafficking machinery from the cell middle, suggesting a competition between the ends and the middle. The cell middle loses this competition and fails cell separation since the requisite digestive enzymes are not properly trafficked. Our candidate screen identifies a role for Rga4, a Cdc42 inhibitor, in growth reactivation at the cell ends. Consistently, we find that the Rga4 distribution pattern along the cortex changes with the cell-cycle stage, displaying a punctate appearance mostly relegated to the cell sides during G2, and a diffuse appearance extending to the cell ends during mitosis. We hypothesize that growth at cell ends requires Rga4 removal from the ends after mitosis as well as MOR pathway activation. To test this, we constitutively activated the MOR pathway in an *rga4Δ* mutant. Cells constitutively activating the MOR pathway often lyse due to premature synthesis and delivery of digestive enzymes to the division site. We find that deleting *rga4* from these cells rescues lysis, and recapitulates the PrESS phenotype by promoting end growth and preventing cell separation. Therefore, we propose that cell-cycle-dependent removal of Rga4 from the cell ends allows local Cdc42 reactivation and polarized growth.

Introduction

Most eukaryotic cells undergo polarized growth to achieve specific shapes that enable them to interact with their environment in a biologically productive manner. Polarized growth requires polarization of growth-promoting signaling networks, actin organization, and membrane trafficking (Etienne-Manneville, 2004; Nance and Zallen, 2011; Ridley, 2006). Polarization is also essential for cytokinesis, the final step in cell division (Albertson et al., 2005; Echard, 2008; Hercyk et al., 2019a; Wang et al., 2016). Since polarized growth and cytokinesis share the same polarization apparatus, they must be temporally distinct events. Accordingly, careful regulation ensures that the cell can alternate between successful growth and division. It is unclear how this is regulated at the molecular level. The major drivers of polarization are highly conserved among eukaryotes (Etienne-Manneville, 2004; Johnson, 1999). For this reason, we use the unicellular fission yeast *Schizosaccharomyces pombe* to establish basic principles about how cells spatiotemporally regulate their polarization machinery.

In fission yeast, cytokinesis involves the formation of an actomyosin ring which then constricts along with an ingressing membrane barrier and septum that physically separates two daughter cells (Cheffings et al., 2016; Pollard, 2010; Pollard, 2014). The septum undergoes maturation and is eventually digested by glucanases, leading to cell separation (Cortes et al., 2016; Garcia Cortes et al., 2016; Sipiczki, 2007). Immediately after cell separation, polarized growth initiates from the old ends, which existed in the previous generation (Mitchison and Nurse, 1985). Once the cells attain a certain size, the new ends, generated as a result of cell division, start to grow by a process called new end take-off (NETO). The Rho GTPase Cdc42 is the master regulator of cell growth and polarity, and is highly conserved among eukaryotes (Etienne-Manneville, 2004; Johnson, 1999). Recently, we have shown that Cdc42 also plays a role in cytokinesis (Hercyk and Das, 2019a; Onwubiko et al., 2020; Wei et al., 2016). Regulation of Cdc42 determines when and where polarization occurs (Das et al., 2009; Etienne-Manneville, 2004). In *S. pombe*, Cdc42 is activated by two Guanine nucleotide exchange factors (GEFs), Scd1 and Gef1 (Chang et al., 1994; Coll et al., 2003), and is inactivated by three GTPase-activating proteins (GAPs), Rga4, Rga6, and Rga3 (Das et al., 2007; Gallo Castro and Martin, 2018; Revilla-Guarinos et al., 2016; Tatebe et al., 2008). Of these, Rga4 appears to be the primary GAP, while Rga6 and Rga3 appear to play minor roles in polarity and sporulation, respectively.

The old ends inactivate Cdc42 during mitosis, and polarized growth consequently stops (Hercyk and Das, 2019b). Once two daughter cells have been generated via cytokinesis at the end of cell division, Cdc42 is reactivated at the old ends and polarized growth resumes (Wei et al., 2016). The bio-probe CRIB-3xGFP specifically binds active Cdc42, and thus is used to identify sites of Cdc42 activation (Tatebe et al., 2008). Using CRIB-3xGFP, it has been shown that Cdc42 is activated at growing cell ends during interphase (Das et al., 2012; Tatebe et al., 2005). Once the cell enters mitosis, active Cdc42 disappears from the cell ends and appears at the division site (Wei et al., 2016). After cell separation, Cdc42 is not immediately activated at a daughter cell's new end, which was created as a result of cell separation. Instead, Cdc42 is first activated at the old end, which is the farthest point from the site of cell division. It is unclear how Cdc42 activation transitions from the division site to the old ends after cell separation.

While much is understood about *how* polarized growth occurs, little is known about the regulation of *when* polarized growth occurs. It has been shown that cell-cycle-dependent signaling pathways temporally segregate cell division and growth phases (Ray et al., 2010; Simanis, 2015). During interphase, the Morphogenesis Orb6 (MOR) pathway promotes cell growth (Nunez et al., 2016; Ray et al., 2010). During cell division, the septation initiation network (SIN) is activated, allowing septum formation (Johnson et al., 2012; Simanis, 2015). Activation of the SIN pathway leads to inactivation of the MOR pathway, thus inhibiting cell growth during septum closure (Ray et al., 2010). Subsequent SIN inactivation allows MOR activation, which leads to cell separation and growth (Gupta et al., 2014; Gupta et al., 2013). This crosstalk between the SIN and MOR signaling pathways thus enforces temporal separation of cytokinesis and cell growth.

The MOR pathway promotes cell separation and polarized growth activation, which occur sequentially. It is unclear how the same signaling pathway sequentially promotes these distinct cellular processes. The MOR pathway involves activating Orb6/NDR kinase, which phosphorylates the exoribonuclease Sts5 (Nunez et al., 2016). Phosphorylation of Sts5 prevents its incorporation into processing bodies (P-bodies), where mRNA is stored or degraded (Nunez et al., 2016). Orb6 activity thus prevents Sts5-dependent degradation of mRNA in the P-bodies, leading to increased protein synthesis. Among the mRNAs spared from degradation are those that encode the glucanases Eng1 and Agn1, and the Ras1 GEF Efc25 (Chen et al., 2019; Nunez et al., 2016). While Eng1 and Agn1 promote septum digestion and cell separation, Efc25-mediated Ras1 activation promotes the localization of the Cdc42 GEF Scd1 to cell ends (Garcia et al., 2005; Lamas et al., 2020a; Martin-Cuadrado et al., 2003; Papadaki et al., 2002). In this way, Orb6 activity promotes cell separation and polarized cell growth. However, constitutively activating the MOR pathway does not lead to constitutive cell growth, but rather to premature cell separation that results in cell lysis (Gupta et al., 2014). This suggests that, once the MOR pathway is activated, cells first undergo separation before old end growth initiates. The nature of the regulation that allows cell separation and growth initiation to occur sequentially is unclear, and is the focus of this study.

Here we investigate how growth is reactivated at the cell ends after cell division. Introducing an artificial cytokinetic delay, we observe that growth activation at the ends occurs independently of cytokinesis completion and cell separation. In keeping with this, we find that Cdc42 activity is timed to resume at the cell ends independent of cell separation. A candidate screen for regulators involved in reactivation of Cdc42 at the cell ends identifies the Cdc42 GAP Rga4. Rga4 always localizes to the cell sides, where it prevents Cdc42 activation (Das et al., 2007; Tatebe et al., 2008). We find that the Rga4 localization pattern along the cortex changes in a cell-cycle-dependent manner. During mitosis, Rga4 appears diffuse and localizes all along the cortex, including the cell ends. We propose that Rga4 localization at the cell ends blocks Cdc42 activation at these ends. Upon mitotic exit, Rga4 is lost from the ends and Cdc42 activity resumes. This suggests that once cell division completes, growth activation at the cell ends occurs when Rga4 is removed from these ends. MOR pathway activation promotes both cell separation and polarized end growth, which normally occur sequentially. Our data

suggest that polarized growth activation occurs once Rga4 is removed from growth sites, allowing these events to occur in sequence. In keeping with our findings, we show that, in mutants constitutively activating the MOR pathway, loss of *rga4* leads to enhanced polarized cell growth. These data suggest that cell-cycle-dependent regulation of Rga4 paired with MOR pathway activation allows cell separation and polarized cell growth to occur sequentially.

Results

Cytokinetic delay results in growth resumption without cell separation.

Since initiation of polarized cell growth at the ends only occurs after cell separation, it stands to reason that polarized growth depends on cell separation. To test this, we used Latrunculin A (LatA) to induce a cytokinetic delay. LatA prevents the polymerization of actin, leading to loss of dynamic actin-based structures (Spector et al., 1983). This treatment therefore causes dissolution of the actomyosin ring, which is only re-assembled once the LatA is washed out and the cells are allowed to recover (Dutartre et al., 1996). This leads to a cytokinetic delay. We treated an asynchronous population of wild type cells with 10μM LatA for 30 minutes and then washed it out. After LatA washout, cells typically take about 45-60 minutes to recover before they start to grow. After recovery, we observed that some cells – about 9% – show a unique phenotype in which they initiate growth at their ends but do not undergo cell separation (Figure 1A,B). We analyzed the timing of end growth initiation with reference to completion of septum closure in these cells. In untreated wild type cells, growth at the ends initiates about 50 minutes after septum closure. However, in cells recovering from LatA treatment, end growth initiates about 6 minutes after septum closure. In some cells, growth initiates even before the completion of septum closure (Figure 1C). Although these cells fail to separate, they enter the next cell cycle and undergo cell division. The septum formed in the second generation separates normally, suggesting that the LatA treatment only impacts the cell cycle in which the cell was treated (Figure 1A, arrow). We call this phenotype the **p**ola**r** **e**longation **s**ans **s**eparation, or PrESS, phenotype. The PrESS phenotype suggests that growth initiation after mitosis occurs independently of cell separation. We also observed that the old ends of PrESS cells grow up to three times as fast as old ends in wild type cells before new end take-off (Supplemental Figure S1).

We asked if the PrESS phenotype occurs simply due to some pleiotropic effect of LatA treatment and not due to a delay in cytokinesis. To test this, we delayed cytokinesis using a temperature-sensitive mutant. We shifted *rng2-D5* mutants to restrictive temperature for 3 hours to block cytokinesis and then reverted back to permissive temperature to enable recovery and growth (Eng et al., 1998; Takaine et al., 2009). Under restrictive conditions, *rng2-D5* mutants stall in cytokinesis due to difficulties constructing a functional actomyosin ring. Upon recovery in permissive conditions, these mutants initiate growth at the old end before cell separation (Figure 1D), as observed in PrESS cells. This shows that the PrESS phenotype is not a pleiotropic effect of LatA treatment, but rather occurs due to a cytokinetic delay, and suggests that growth initiation occurs independently of cell separation.

Cdc42 activation at cell ends is cell-cycle-dependent.

Only a subset of asynchronous cells exhibits the PrESS phenotype upon recovery from LatA treatment. We asked if this is because the PrESS phenotype only occurs in cells that are in a certain cell cycle stage. To address this, we imaged cells at various cell-cycle stages before, during, and after LatA treatment. We accomplished this by affixing the cells to the imaging dish using lectin (Tay et al., 2018), and performing LatA

treatment and washout within the dish itself. Cells in lectin-coated dishes tend to grow slower than normal, but do not show any significant growth defects. We found that mitotic cells treated with LatA show the PrESS phenotype after recovery (Figure 2Aii), and that cells treated during interphase or G1/S separate normally (Figure 2Ai, iii). When treated with LatA, cells in anaphase continue to proceed through mitosis, as detected with the spindle pole body marker Sad1-mCherry. However, the actomyosin ring disassembles, as marked by the type 2 myosin light chain Rlc1-tdTomato. After LatA washout, the actomyosin ring reassembles and then proceeds to constrict along with septum ingression (Figure 2Aii, arrowhead). However, instead of undergoing septum digestion and cell separation, these cells grow from the ends, thus displaying the PrESS phenotype. These observations show that the PrESS phenotype arises from cells that are in mitosis at the time of LatA treatment.

To confirm this, we synchronized *cdc25-22* cells by shifting them to restrictive temperature and arresting them in late G2 (Fantes and Nurse, 1978; Tormos-Perez et al., 2016). Upon shifting back to permissive temperature, the synchronized cells enter mitosis. We took samples of cells released from arrest at regular time intervals. The cell-cycle stage of these cells was determined by Phalloidin and DAPI staining after formaldehyde fixation of a fraction of the samples. Cells in G2 show a single nucleus with actin mainly at the cell ends, and in mitosis show a dividing nucleus with an actin ring at the cell middle. In G1/S, the cell middle shows a septum instead of an actin ring, with a single nucleus in each sister cell. The remaining fractions of the samples were treated with LatA like before and allowed to recover. We found that cells treated with LatA during late G2 went on to septate and divide normally (Figure 2B). Cells released from restrictive temperature for 40 minutes were in mitosis at the time of LatA treatment. These cells almost exclusively went on to display the PrESS phenotype. Cells released from restrictive temperature for 80 minutes were septated at the time of LatA treatment, as evidenced by lack of an actomyosin ring and divided nuclei. These cells successfully separated after recovery and therefore did not display the PrESS phenotype. These findings suggest that the PrESS phenotype is cell-cycle-dependent and only occurs in cells that are in mitosis at the time of LatA treatment.

PrESS cells activate Cdc42 at the growing ends at the expense of the division site.

Why do PrESS cells fail to separate? Cell separation requires the formation of a tri-layered septum which is subsequently digested by glucanases (Cortes et al., 2016; Garcia Cortes et al., 2016; Sipiczki, 2007). The septum is comprised of a primary septum flanked by secondary septum. Glucanases are delivered to the cortex at the outer edge of the septum barrier to digest the primary septum and allow separation. Separation defects occur either due to lack of primary septum formation or improper delivery of the glucanases. We asked if separation failure in PrESS cells is due to improper primary septum formation. To test this, we performed electron microscopy of cells recovering from LatA treatment. Electron microscopy shows that the non-separating septum in a PrESS cell is constructed properly, displaying a distinct tri-layer similar to that observed in untreated cells (Supplemental Figure S2A). These cells also

showed proper recruitment of the primary septum-synthesizing enzyme Bgs1 during septation (Supplemental Figure S2B). Moreover, the original septum in a PrESS cell often goes on to separate, albeit after a prolonged delay (Supplemental Figure S2C). The septum therefore appears competent for separation, suggesting that cell separation does not fail in PrESS cells due to a structural defect in the septum.

Cell separation failure can occur due to improper delivery of the septum-digesting glucanases to the division site (Garcia Cortes et al., 2016). Normally, once delivered to the division site, glucanases are secreted to the outer edge of the membrane barrier, where they digest the primary septum. We asked if PrESS cells' failure to undergo cell separation was due to improper delivery of these glucanases. To test this, we imaged the glucanases Eng1 and Agn1 (Dekker et al., 2004; Martin-Cuadrado et al., 2003) at the division site of PrESS cells. In untreated cells, Eng1 and Agn1 localize to the outer edge of the membrane barrier and thus appear as a ring when viewed laterally (Figure 3A) (Martin-Cuadrado et al., 2005). In PrESS cells, Eng1 and Agn1 appear as a patchy disc all over the membrane barrier and do not localize to the outer edge (Figure 3A). This altered localization pattern is similar to that observed in mutants that fail to deliver glucanases and thus fail to undergo cell separation (Martin-Cuadrado et al., 2005; Perez et al., 2015; Santos et al., 2005; Wang et al., 2015). This suggests that cell separation failure in PrESS cells is due to improper delivery of the glucanases required for septum digestion.

We have recently reported that the glucanases do not localize properly to the outer edge of the membrane barrier in a hypomorphic mutant of the small GTPase Cdc42 (Onwubiko et al., 2020). Cdc42 activity stops at the cell ends during mitosis and transitions to the division site during cytokinesis (Merla and Johnson, 2000; Rincon et al., 2007; Wei et al., 2016). Once the cell separates, Cdc42 activity returns to the cell ends and growth resumes (Figure 3B, upper panel, asterisks). Competition for Cdc42 activity occurs between the two growing ends of a fission yeast cell (Das et al., 2012). Normally, Cdc42 is not activated at the old ends of the daughter cells until after cell separation has occurred (Figure 3B). However, in PrESS cells, we find that Cdc42 activation occurs earlier at these ends (Figure 3B, lower panel, asterisks), while it gradually fades away from the intact septum (Figure 3B, arrowhead). We hypothesize that this is indicative of a competition in PrESS cells between the old ends and the septum. These sites ordinarily do not attempt to activate Cdc42 concurrently, and thus do not compete with each other. However, since PrESS cells experience a cytokinetic delay, these sites simultaneously attempt to activate Cdc42, resulting in a competition for Cdc42 activity. The site of cell division fails in this competition, likely resulting in cell separation failure. These conjoined cells eventually enter the next cell cycle and show normal Cdc42 activation at the cell ends during interphase and at the new division site during cytokinesis. This shows that subsequent cell cycles progress normally in PrESS cells.

Next, we analyzed the localization of the Cdc42 GEF Scd1 and its scaffold Scd2 (Chang et al., 1994). During cytokinesis, Scd1 and Scd2 localize to the division membrane barrier and remain at that site until cell separation (Hercyk et al., 2019b; Hirota et al., 2003). In PrESS cells, we find that Scd1-3xGFP and Scd2-GFP are lost from the division site (Figure 3C, arrowhead) and appear at the cell ends, where they become

enriched over time (Figure 3C, asterisk). Cdc42 is required for membrane trafficking events (Estravis et al., 2012; Estravis et al., 2011; Harris and Tepass, 2010; Murray and Johnson, 2001). With dwindling Cdc42 activity at the septum, we would expect a disruption of membrane trafficking. To test this, we analyzed the recruitment of the type 5 myosin Myo52 to the division site (Win et al., 2001). Indeed, in PrESS cells, we observe that Myo52-tdTomato localization gradually favors the cell ends over the septum (Figure 3C). Together, these findings suggest that Cdc42 activity, and consequently the membrane trafficking apparatus, transition to the cell ends from the division site. This leads to cell separation failure due to improper delivery of the glucanases that digest the primary septum.

A candidate screen to identify cell-cycle-dependent regulators of Cdc42 activation

Next, we wanted to identify how Cdc42 is regulated in a cell-cycle-dependent manner at the cell ends. We hypothesized that a Cdc42 regulator is under cell cycle control. Once cell division completes, this regulator enables Cdc42 activation at the ends. To identify this regulator, we performed a candidate screen of known and potential mutants of Cdc42 regulators, listed in Table S2. We measured the frequency of the PrESS phenotype in these mutants. Variation in cell size of the different mutants was taken into account in computing the PrESS frequency, as described in the materials and methods. We observed the PrESS phenotype in all but one of the mutants analyzed. The PrESS phenotype did not occur in the *cdc16-116* mutant (Table S2). Cdc16 is a GAP that inactivates the SIN pathway. This hypomorphic *cdc16-116* mutant shows constitutive SIN activation that leads to continual septation and absence of cell growth (Schmidt et al., 1997). This suggests that the PrESS phenotype occurs as long as a cell is capable of growth. It is reported that Cdc42 activation in LatA-treated cells is regulated by the MAP kinase Sty1 (Mutavchiev et al., 2016; Toda et al., 1996). We asked if the PrESS phenotype is a Sty1-dependent stress response. The PrESS phenotype persisted in *sty1Δ* mutants, suggesting that this phenotype is not a stress response to LatA treatment (Supplementary figure S3A). Cell polarity in fission yeast depends on actin as well as the microtubule cytoskeleton. The microtubule-dependent Tea1 protein localizes polarity markers to the cell ends (Feierbach et al., 2004; Glynn et al., 2001). However, *tea1Δ* mutants show the PrESS phenotype after recovery from LatA treatment. This suggests that the PrESS phenotype is independent of the microtubule-associated polarity markers (Supplementary figure S3C).

Polarized Cdc42 activation depends on Ras1 GTPase, which promotes polarized localization of the Cdc42 GEF Scd1 (Chang et al., 1994; Chen et al., 2019; Lamas et al., 2020b). However, *ras1Δ* mutants continue to display the PrESS phenotype after recovery from LatA treatment (Supplementary figure S3B). In addition, loss of either of the partially redundant GEFs, Scd1 and Gef1, does not lead to reduced PrESS frequency (Figure 4A, B). Moreover, PrESS cells in *scd1Δ* appear more polarized as compared to untreated *scd1Δ* cells. This suggests that cell-cycle-dependent activation of Cdc42 at the ends is not dependent on a specific GEF, and that as long as a GEF is available, Cdc42 at the cell ends will be activated. We find that *gef1Δ* shows a higher

PrESS frequency than wild type. We have previously shown that in *gef1Δ* cells, the old end competes with the new end for Cdc42 more effectively than wild type. Thus, in *gef1Δ* mutants, a robust old end can explain the higher PrESS frequency we observe.

Next, we analyzed the PrESS phenotype in deletion mutants of the Cdc42 GAPs Rga4 and Rga6. The Cdc42 GAPs inactivate Cdc42 at the cortex (Das et al., 2007; Revilla-Guarinos et al., 2016; Tatebe et al., 2008). We did not see any change in the PrESS frequency of *rga6Δ* cells. In contrast, *rga4Δ* shows a significantly higher incidence of the PrESS phenotype compared to wild type cells ($p<0.05$) (Figure 4C, D). *rga4Δ* cells are wider and shorter than wild type (Das et al., 2007). Consistently, *rga4Δ* PrESS cells are wider and shorter compared to wild type PrESS cells. The increased PrESS frequency we observe in *rga4Δ* cells suggests that, after cell division, old end activation involves regulation of Rga4.

Rga4 localization is regulated in a cell-cycle-dependent manner

Since our data suggest a role for Rga4 in regulating Cdc42 at the cell ends after cell division, we asked if Rga4 itself is regulated in a cell-cycle-dependent manner. Rga4 localizes mainly to the cell sides, where it blocks Cdc42 activation (Das et al., 2007; Tatebe et al., 2008). In wild type cells, we observe that Rga4-GFP localizes mostly to the cell sides during interphase (Figure 5A). As the cell enters division, Rga4-GFP can be found not only at the cell sides, but also at the ends. Time-lapse imaging of Rga4-GFP (10 sec intervals for 1 minute) indicates that Rga4-GFP at the cell ends is dynamic in nature (Supplementary figure S4A). A time-lapse projection of Rga4-GFP (10 sec intervals for 5 minutes) shows enhanced signal at the cell ends in mitotic cells as compared to interphase cells (Figure 5B, asterisk). In pre-NETO cells, in which the new end does not grow, Rga4-GFP is often visible at that end. However, only 50% of interphase cells show any Rga4-GFP signal at the old ends (Figure 5D). In early anaphase, on average 89.3% of cells show Rga4-GFP at the old ends. As mitosis progresses and cells enter late anaphase, 65% of cells show Rga4-GFP at these ends. Finally, in G1/S phase, 56.7% of cells show Rga4-GFP at these ends. Rga4-GFP is not suited for long-term live-cell imaging since it bleaches rapidly. Nevertheless, we tried to capture whether Rga4-GFP is observable at the cell ends during early mitosis. The spindle pole body marker Sad1-mCherry is used to time mitotic progression. Using Sad1-mCherry and the actomyosin ring marker Rlc1-tdTomato, we observed Rga4-GFP localization at the cell ends during early mitosis (Figure 5C, arrows).

We further observe that not only the localization, but also the distribution, of Rga4-GFP along the cortex changes throughout the cell cycle. In G2, Rga4-GFP appears as puncta dispersed along the cell sides (Figure 5A). During mitosis, it appears to be spread more homogenously along the cortex (Figure 5A, bracket). We quantified these changes by measuring the coefficient of variation of Rga4-GFP distribution along the cortex. The higher the coefficient of variation, the less homogenous the distribution of Rga4-GFP. We find that the coefficient of variation is higher during G2 than it is during cell division, reflecting our observation that Rga4-GFP appears more punctate during G2 and more diffuse during mitosis (Figure 5E). The coefficient of variation drops in cells undergoing mitosis and appears to increase again in cells in G1/S. This suggests

that Rga4-GFP appears more punctate along the cortex in G2. In mitotic cells, the distribution of Rga4-GFP along the cortex is more homogenous, and this gradually reverts back to a more punctate appearance as the cells enter the G1/S phase.

Our analysis indicates that Rga4 localization and distribution changes through different cell-cycle stages. We asked if these changes are indeed cell-cycle-dependent. To test this, we analyzed the localization pattern of Rga4-GFP in the *cdc2-as* mutant. *cdc2-as* is an analog-sensitive mutation in the mitotic kinase Cdk1 which allows specific inhibition of its kinase activity upon addition of the inhibitor 1NM-PP1 (Aoi et al., 2014). In untreated and thus asynchronous *cdc2-as* cells, the Rga4-GFP distribution pattern is similar to that observed in control cells (Supplemental Figure S4B, Figure 5E). Next, we synchronized *cdc2-as* cells by adding the inhibitor 1NM-PP1. After the cells arrested in G2, we washed out the analog to allow release into mitosis. Distribution of Rga4-GFP along the cortex was analyzed in cells at different cell cycle stages. Cells arrested in G2, when Cdc2 activity is inhibited, show a high coefficient of variation, suggesting a more punctate Rga4-GFP distribution (Figure 5F, G). Approximately 20 minutes after removal of the inhibitor, the cells were in early anaphase. Under these conditions, the coefficient of variation of Rga4-GFP distribution is significantly reduced, suggesting a more homogenous distribution (Figure 5F, G). Similarly, cells in late anaphase, about 40 minutes after release, also show a decreased coefficient of variation of Rga4-GFP distribution. The coefficient of variation in *cdc2-as* cells synchronized in G1/S (~70 minutes after release) is higher than that in mitotic cells, suggesting that the punctate distribution reappears after mitotic exit. However, in asynchronous cells, the coefficient of variation in G1/S is lower than that in G2 (Figure 5E). It is possible that, in G1/S, Rga4-GFP distribution gradually returns to a more puncta-like appearance, similar to G2. This change is likely better captured in synchronized cells. In cell-cycle-arrested *cdc2-as* cells, which are larger than wild type cells, Rga4-GFP was not clearly visible at the cell ends. It is possible that the increased cell size of these arrested cells leads to a decrease in the local concentration of Rga4-GFP at the ends.

Rga4 removal allows polarized growth activation after cell division.

Our data suggest that Cdc42 regulation at the cell ends is cell-cycle-dependent and shows that loss of *rga4* enhances PrESS frequency. Moreover, we find that localization of Rga4 to cell ends increases during mitosis when Cdc42 activation at those ends is known to decline. We propose that two elements are necessary for polarized growth to occur: MOR pathway activation leading to protein synthesis, as well as Cdc42 activation at the cell ends. During mitosis, the MOR pathway is inactive and Rga4 is present at the ends, and thus growth does not occur. As cell division completes, the MOR pathway becomes active and the cell ends lose Rga4, enabling local Cdc42 activation. In PrESS cells, cytokinesis is delayed, but activation of the MOR pathway and Cdc42 activation at the ends are triggered as normal, resulting in polarized growth. We should thus be able to recapitulate the PrESS phenotype in cells both constitutively activating the MOR pathway and allowing Cdc42 activation at the cell ends even without delaying cytokinesis via LatA treatment. Constitutive activation of the MOR pathway via expression of the Nak1-Mor2 fusion protein leads to premature protein synthesis during

cell division (Gupta et al., 2014). This includes the glucanases that are then prematurely delivered to the incomplete septum barrier, resulting in cell lysis (Figure 6A, arrows). We hypothesized that if the cell ends were instead able to activate growth, the glucanases would not be delivered to the division site, resulting in a PrESS-like phenotype. Based on our previous observations, we should accomplish this by deleting *rga4* in a mutant constitutively activating the MOR pathway. Since Nak1-Mor2-expressing cells undergo cell lysis resulting in cell death, they display a low optical density (Gupta et al., 2014). We find that *rga4Δ* cells expressing Nak1-Mor2 for 16 hours do not undergo cell lysis, and display higher optical density over time similar to that in cells repressing Nak1-Mor2. (Figure 6B). Moreover, these cells fail to undergo cell separation and continue to grow from their ends, similar to PrESS cells (Figure 6A, arrowhead). Note that *rga4Δ* cells are normally capable of cell separation, and thus failure to separate with Nak1-Mor2 expression is due to premature growth at the old ends. We thus propose that lack of Rga4 at the cell ends allows the ends to better compete for growth machinery, preventing localization of these proteins to the division site. This suggests that under normal conditions, after MOR pathway activation, cell end growth occurs after Rga4 removal from those ends.

Discussion

Although much is known about how polarized growth occurs in fission yeast, it is unclear how polarized growth resumes at the old ends after cell division completes. Specifically, it is unknown how Cdc42 activity transitions from the division site to the old ends to drive polarized growth. Since Cdc42 activation at the old end normally does not occur until after completion of cell separation, it would appear as if separation itself allows Cdc42 activity at the old end. However, here we show that Cdc42 activation at the old end is independent of cell separation and rather is cell-cycle-dependent.

The MOR pathway promotes cell separation and polarized growth after cell division (Chen et al., 2019; Gupta et al., 2014; Nunez et al., 2016; Ray et al., 2010). The final step in cell division, cytokinesis, involves actomyosin ring formation and subsequent constriction in coordination with septum formation and membrane invagination (Cheffings et al., 2016; Garcia Cortes et al., 2016; Pollard, 2010). After ring constriction, the septum matures to form a tri-layer, a primary septum flanked by secondary septum (Cortes et al., 2016; Garcia Cortes et al., 2016). MOR pathway activation allows synthesis of glucanases which are delivered to the outer edge of the membrane barrier to precisely digest the primary septum, resulting in cell separation (Martin-Cuadrado et al., 2005; Nunez et al., 2016; Santos et al., 2005). Once septum digestion starts, Cdc42 activity transitions to the old ends and polarized growth initiates. It was unclear how the MOR pathway sequentially enables cell separation at the division site followed by growth at the ends. Constitutively activating the MOR pathway leads to premature cell separation during division, which is caused by unregulated delivery of the glucanases and results in lysis. Here we report the novel PrESS phenotype in which polarized cell growth initiates during cytokinesis. Our data suggest that, in these cells, Cdc42 is activated at the ends before cell separation. Activation of Cdc42 at the ends in these cells siphons Cdc42 activity from the division site. This prevents delivery of glucanases to the division site and allows the ends to grow. This indicates that under normal conditions, Cdc42 at the ends is inhibited while the cell successfully undergoes separation. The ends are able to activate Cdc42 only after cell separation completes, even as the MOR pathway is active throughout this stage. These observations together suggest that, in addition to MOR activation, another pathway regulates Cdc42 at the ends after division.

Our results indicate that Rga4 is regulated at the cell ends during mitosis. We show that Rga4 localizes all the way to the cell ends during mitosis, instead of being restricted to the cell sides (Das et al., 2007). It is possible that Rga4 at the ends during mitosis blocks Cdc42 activation. Accordingly, we hypothesize that, in the absence of *rga4*, cells should initiate growth at the old ends during division as long as protein synthesis is active, thus recapitulating the PrESS phenotype. Indeed, in cells constitutively activating the MOR pathway, loss of *rga4* leads to old end growth and cell separation failure in a recapitulation of the PrESS phenotype, thus supporting our hypothesis.

How does Rga4 localize to the cell ends during mitosis? Rga4 typically localizes to the cell sides during G2 and is excluded from the cell ends. During this phase, Rga4 appears as distinct puncta dotted along the cell sides. However, during mitosis, Rga4 appears more diffuse along the cortex and extends all the way to the cell ends. Cells

arrested in G2 show distinct puncta-like Rga4 distribution at the cell sides. Upon release, when the cells enter mitosis, Rga4 appears diffuse at the cortex. It is unclear how Rga4 localization is regulated during mitosis. Rga4 could be a direct target of the mitotic kinase Cdk1 or of an unknown cell-cycle-dependent regulatory module. In another study, Rga4 has been identified as a target of Cdk1 kinase activity, however the physiological significance of this interaction is unknown (Swaffer et al., 2016). We are currently investigating the nature of cell-cycle-dependent Rga4 regulation during mitosis in fission yeast. It is not clear how Rga4 is removed from the cell ends at the end of cell division. Rga4 lingers at the ends well after activation of the anaphase-promoting complex, which promotes Cdk1 inactivation. It is possible that Rga4 undergoes some modification that gradually leads to its removal from the ends. This could be mediated by a phosphatase, by turnover of Rga4, or by an unknown mechanism. In budding yeast, CDKs Pho85 and Cdc28 phosphorylate the GAP Rga2 to restrain its activity and promote polarized growth (Sopko et al., 2007). Another study in budding yeast has shown that the G1-cyclin CDKs promote Cdc42 activation (McCusker et al., 2007). G1-cyclin-CDK promotes Cdc42 activation via the GEF Cdc24, thus allowing bud growth. In contrast, our findings suggest a mitosis-dependent negative regulation of Cdc42. It is unclear if the G1-cyclin-CDK complex in fission yeast also regulates Cdc42.

While we find that Rga4 localizes to the cell ends during mitosis, it should be noted that loss of *rga4* alone does not enable Cdc42 activation at this stage. This is probably because, even in the *rga4* mutants, the MOR pathway is inhibited during mitosis. Thus, MOR inactivation is likely sufficient to inhibit Cdc42 activation at the ends. However, after division, Cdc42 activation at the cell ends requires both removal of Rga4 from the cell ends and MOR activation. A recent preprint has shown that presence of the GAPs at the cortex prevents Cdc42 activation at those sites even when the scaffold Scd2, which recruits Scd1 to the cortex, localizes to those sites (Lamas et al., 2020b). Another preprint suggests that Cdc42 GAP levels in daughter cells determine the pattern of polarized growth in those cells (Pino et al., 2020). This report and our findings together indicate that removal of Rga4 from the cell ends after cell division is necessary to promote Cdc42 activation at these ends.

The MOR pathway is necessary for cell separation as well as polarized cell growth. Once the MOR pathway is activated, cells first undergo separation and then initiate polarized growth at the old ends. Based on our findings, we propose a model to describe how polarized cell growth is initiated after cell separation (Figure 7). Cdc42 activity from the ends declines once the cell enters mitosis and is completely lost from these sites as mitosis progresses. At this stage, Rga4 no longer appears as distinct puncta along the cell sides. Rather, it displays diffuse distribution along the cortex which extends to the cell ends. After the metaphase checkpoint, the cell enters anaphase, and the SIN is activated while the MOR pathway is inactivated (Simanis, 2015). Polarized cell growth at the ends stops at this stage. Once cytokinesis is complete, the SIN is inactivated and MOR pathway is activated, allowing synthesis of proteins necessary for cell separation and polarized growth. As the cells separates, Rga4 is gradually lost from the cell ends and its punctate distribution is restored. After removal of Rga4 from the cell ends, they initiate growth. In LatA-treated cells, cytokinesis is delayed while mitosis progresses. In such cells, Rga4 is removed from the cell ends on time, leading to Cdc42

activation and growth at these sites while cytokinesis still progresses, thus resulting in the PrESS phenotype.

Through an artificial cytokinetic delay, we have uncovered a basic cellular principle which ensures that growth occurs at an appropriate time. It is telling that growth is carefully suppressed during mitosis, and that a cytokinetic delay will not prevent growth. Cdc42 activity is thus regulated based on a mitotic timer without regard to completion of cytokinesis. This especially makes sense in the context of pseudohyphal growth, which fission yeast typically undergo in nature. Our findings suggest that the timing of growth initiation, while cell-cycle-dependent, is programmed to occur after cell separation. Our work provides a better understanding of how growth initiates after mitosis in fission yeast. An elegant cell-cycle-dependent system causes a subtle but effective localization change, controlling the timing of Cdc42 activation at the cell ends.

Materials and Methods

Strains and cell culture

The *Schizosaccharomyces pombe* strains used in this study are listed in Table S1. Cells were cultured in yeast extract (YE) medium and grown exponentially at 25°C unless otherwise specified (Moreno et al., 1991). Cells were grown for at least three days before imaging.

Latrunculin A treatments

Cells were treated with 10μM Latrunculin A (LatA) (Sigma-Aldrich #428021) for 30 minutes. The cells were washed twice with the appropriate media, switched to a fresh tube, and washed a third time.

PrESS frequency measurements

Wild type, *scd1Δ* and *gef1Δ* were all imaged on the same three days, and wild type and *rga4Δ* were both imaged on the same three days. Cells were LatA-treated and washed as described above, and then imaged immediately after wash as well as every hour after wash for five hours. Untreated cells were imaged as a control for each strain. The length of each septated cell was measured, and the average and standard deviation were calculated. Any cell measured to be longer than two standard deviations more than the average for the corresponding untreated sample was counted as a PrESS cell. The reported peaks are the actual PrESS percentages minus the control PrESS percentage, which was always under 1%.

cdc25-22 synchronization

Strains synchronized using the *cdc25-22* temperature-sensitive mutation were shifted to restrictive temperature, 36°C, for four hours and then shifted back to permissive temperature, 25°C.

Cdc2-as inhibition and synchronization

Synchronization of cells containing *cdc2-as* was achieved via addition of 1NM-PP1 (Toronto Research Chemicals #A603003) to a concentration of 500nM for four hours. Cells were then washed three times with YE media to remove the inhibitor.

Growth curve

Cells were grown at 25°C. To achieve plasmid expression, thiamine was washed out immediately before the experiment began. Cells were diluted to an O.D. of 0.01 and loaded into a 96-well plate, which was read by a BioTek Cytation 5 plate reader. O.D.

measurements were collected every fifteen minutes for 48 hours. During the experiment, the cells were maintained at 29°C, with shaking.

Analysis of Rga4 distribution

In ImageJ, for both sides of each cell in a single plane, a line was drawn along the cell side. Then, a plot profile was generated, and the intensity values were averaged to give an average coefficient of variation for Rga4-GFP distribution along the sides.

Statistical tests

GraphPad Prism was used to perform statistical tests. A Student's t-test (two-tailed, unequal variance) was used to determine significance when comparing two samples. When comparing three or more samples, one-way ANOVA was used alongside Tukey's multiple comparisons, unless otherwise mentioned.

Microscopy

Imaging was performed at room temperature (23-25°C). We used an Olympus IX83 microscope equipped with a VTHawk two-dimensional array laser scanning confocal microscopy system (Visitech International, Sunderland, UK), electron-multiplying charge-coupled device digital camera (Hamamatsu, Hamamatsu City, Japan), and a 100x/1.49 numerical aperture UAPO lens (Olympus, Tokyo, Japan). We also used a spinning disk confocal microscope system with a Nikon Eclipse inverted microscope with a 100x /1.49 numerical aperture lens, a CSU-22 spinning disk system (Yokogawa Electric Corporation), and a Photometrics EM-CCD camera. Images were acquired with MetaMorph (Molecular Devices, Sunnyvale, CA) and analyzed with ImageJ (National Institutes of Health, Bethesda, MD (Schneider et al., 2012). For still and z-series imaging, the cells were mounted directly on glass slides with a #1.5 coverslip (Fisher Scientific, Waltham, MA) and imaged immediately, and with fresh slides prepared every ten minutes. Z-series images were acquired with a depth interval of 0.4 µm. For time-lapse images, cells were placed in 3.5mm glass-bottom culture dishes (MatTek, Ashland, MA) and overlaid with YE medium containing 0.6% agarose and 100 µM ascorbic acid as an antioxidant to minimize toxicity to the cell, as reported previously.

For cells attached to MatTek dishes with lectin, we first let 10µL of 1mg/1mL lectin (Sigma-Aldrich #L1395) incubate in the center of the dish at room temperature for 30 minutes. Then, we washed with 1mL of YE media three times to remove excess lectin not adhered to the dish. We spun down 1mL of cells at an O.D. of about 0.5 and removed all 950µL of the supernatant, then resuspended and pipetted the remaining 50µL into the center of the dish. We then rinsed the dish with YE media three times to remove excess cells not adhered to the lectin. YE media was subsequently kept in the dish at all times to prevent cell starvation, except during short time periods during washes and drug treatments.

Electron microscopy

Wild type cells in late G2 were selected from a sucrose gradient. These cells were treated with 10μM LatA for 30 minutes and then washed three times with YE media. The untreated wild type control cells were not selected from a sucrose gradient. Both samples were washed in sterile water three times and fixed in 2% potassium permanganate for one hour at room temperature. They were again washed three times in sterile water and then resuspended in 70% ethanol and incubated overnight at room temperature. Dehydration was achieved via an ethanol series at room temperature: in order, two 15-minute incubations in 70% ethanol, two 15-minute incubations in 95% ethanol, and finally three 20-minute incubations in 100% ethanol. The cells were then incubated for 30 minutes in propylene oxide, followed by a 1-hour incubation in a 1:1 mixture of propylene oxide and Spurr's resin, and lastly two 1-hour incubations in neat Spurr's resin. The cells were pelleted via centrifugation and the supernatant carefully removed in between each incubation. The cells were transferred into small plastic tubes, and fresh Spurr's resin was layered above to the top of the tube. The two resulting tubes were incubated at 60°C overnight. Sectioning yielded approximately 100nm sections. Sections were post-stained with lead citrate for 8 minutes. Sections were washed by dunking in three sequential beakers of sterile water thirty times each, and allowed to dry on filter paper. Samples were imaged with the Zeiss Dual Beam FIB/SEM microscope at the Joint Institute for Advanced Materials (Knoxville, Tennessee). All images were collected at 15kV.

Acknowledgements

We thank Brian Hercyk, Udo Onwubiko, Bethany Campbell, and Marcus Harrell for discussions and feedback; Kathy Gould, Sophie Martin, Jonathan Millar, Pilar Perez, and Fulvia Verde for strains; Dannel McCollum for plasmids; and John Dunlap for electron microscopy.

This work was funded by an NIH-NIGMS R01 grant (#1R01GM136847-01) awarded to MD. JRR was awarded an NSF Graduate Research Fellowship Program (GRFP) (#1452154), as well as the NIH's Initiative for Maximizing Student Development (IMSD) (#R25GM086761).

References

Albertson, R., B. Riggs, and W. Sullivan. 2005. Membrane traffic: a driving force in cytokinesis. *Trends in cell biology*. 15:92-101.

Aoi, Y., S.A. Kawashima, V. Simanis, M. Yamamoto, and M. Sato. 2014. Optimization of the analogue-sensitive Cdc2/Cdk1 mutant by in vivo selection eliminates physiological limitations to its use in cell cycle analysis. *Open biology*. 4.

Chang, E.C., M. Barr, Y. Wang, V. Jung, H.P. Xu, and M.H. Wigler. 1994. Cooperative interaction of S. pombe proteins required for mating and morphogenesis. *Cell*. 79:131-141.

Cheffings, T.H., N.J. Burroughs, and M.K. Balasubramanian. 2016. Actomyosin Ring Formation and Tension Generation in Eukaryotic Cytokinesis. *Current biology : CB*. 26:R719-R737.

Chen, C., M. Rodriguez Pino, P.R. Haller, and F. Verde. 2019. Conserved NDR/LATS kinase controls RAS GTPase activity to regulate cell growth and chronological lifespan. *Molecular biology of the cell*. 30:2598-2616.

Coll, P.M., Y. Trillo, A. Ametzazurra, and P. Perez. 2003. Gef1p, a new guanine nucleotide exchange factor for Cdc42p, regulates polarity in Schizosaccharomyces pombe. *Molecular biology of the cell*. 14:313-323.

Cortes, J.C., M. Ramos, M. Osumi, P. Perez, and J.C. Ribas. 2016. Fission yeast septation. *Communicative & integrative biology*. 9:e1189045.

Das, M., T. Drake, D.J. Wiley, P. Buchwald, D. Vavylonis, and F. Verde. 2012. Oscillatory Dynamics of Cdc42 GTPase in the Control of Polarized Growth. *Science*. 337:239-243.

Das, M., D.J. Wiley, X. Chen, K. Shah, and F. Verde. 2009. The conserved NDR kinase Orb6 controls polarized cell growth by spatial regulation of the small GTPase Cdc42. *Current biology : CB*. 19:1314-1319.

Das, M., D.J. Wiley, S. Medina, H.A. Vincent, M. Larrea, A. Oriolo, and F. Verde. 2007. Regulation of cell diameter, For3p localization, and cell symmetry by fission yeast Rho-GAP Rga4p. *Molecular biology of the cell*. 18:2090-2101.

Dekker, N., D. Speijer, C.H. Grun, M. van den Berg, A. de Haan, and F. Hochstenbach. 2004. Role of the alpha-glucanase Agn1p in fission-yeast cell separation. *Molecular biology of the cell*. 15:3903-3914.

Dutartre, H., J. Davoust, J.P. Gorvel, and P. Chavrier. 1996. Cytokinesis arrest and redistribution of actin-cytoskeleton regulatory components in cells expressing the Rho GTPase CDC42Hs. *Journal of cell science*. 109 (Pt 2):367-377.

Echard, A. 2008. Membrane traffic and polarization of lipid domains during cytokinesis. *Biochemical Society transactions*. 36:395-399.

Eng, K., N.I. Naqvi, K.C. Wong, and M.K. Balasubramanian. 1998. Rng2p, a protein required for cytokinesis in fission yeast, is a component of the actomyosin ring and the spindle pole body. *Current biology : CB*. 8:611-621.

Estravis, M., S. Rincon, and P. Perez. 2012. Cdc42 regulation of polarized traffic in fission yeast. *Communicative & integrative biology*. 5:370-373.

Estravis, M., S.A. Rincon, B. Santos, and P. Perez. 2011. Cdc42 regulates multiple membrane traffic events in fission yeast. *Traffic*. 12:1744-1758.

Etienne-Manneville, S. 2004. Cdc42--the centre of polarity. *Journal of cell science*. 117:1291-1300.

Fantes, P.A., and P. Nurse. 1978. Control of the timing of cell division in fission yeast. Cell size mutants reveal a second control pathway. *Exp Cell Res*. 115:317-329.
Feierbach, B., F. Verde, and F. Chang. 2004. Regulation of a formin complex by the microtubule plus end protein tea1p. *The Journal of cell biology*. 165:697-707.
Gallo Castro, D., and S.G. Martin. 2018. Differential GAP requirement for Cdc42-GTP polarization during proliferation and sexual reproduction. *The Journal of cell biology*. 217:4215-4229.
Garcia Cortes, J.C., M. Ramos, M. Osumi, P. Perez, and J.C. Ribas. 2016. The Cell Biology of Fission Yeast Septation. *Microbiology and molecular biology reviews : MMBR*. 80:779-791.
Garcia, I., D. Jimenez, V. Martin, A. Duran, and Y. Sanchez. 2005. The alpha-glucanase Agn1p is required for cell separation in Schizosaccharomyces pombe. *Biol Cell*. 97:569-576.
Glynn, J.M., R.J. Lustig, A. Berlin, and F. Chang. 2001. Role of bud6p and tea1p in the interaction between actin and microtubules for the establishment of cell polarity in fission yeast. *Current biology : CB*. 11:836-845.
Gupta, S., M. Govindaraghavan, and D. McCollum. 2014. Cross talk between NDR kinase pathways coordinates cytokinesis with cell separation in Schizosaccharomyces pombe. *Eukaryotic cell*. 13:1104-1112.
Gupta, S., S. Mana-Capelli, J.R. McLean, C.T. Chen, S. Ray, K.L. Gould, and D. McCollum. 2013. Identification of SIN pathway targets reveals mechanisms of crosstalk between NDR kinase pathways. *Current biology : CB*. 23:333-338.
Harris, K.P., and U. Tepass. 2010. Cdc42 and vesicle trafficking in polarized cells. *Traffic*. 11:1272-1279.
Hercyk, B., and M. Das. 2019a. Rho Family GTPases in Fission Yeast Cytokinesis. *Communicative & integrative biology*. 12:171-180.
Hercyk, B.S., and M.E. Das. 2019b. F-BAR Cdc15 Promotes Gef1-mediated Cdc42 Activation During Cytokinesis and Cell Polarization in *S. pombe*. *Genetics*.
Hercyk, B.S., U.N. Onwubiko, and M.E. Das. 2019a. Coordinating septum formation and the actomyosin ring during cytokinesis in Schizosaccharomyces pombe. *Molecular microbiology*. 112:1645-1657.
Hercyk, B.S., J. Rich-Robinson, A.S. Mitoubsi, M.A. Harrell, and M.E. Das. 2019b. A novel interplay between GEFs orchestrates Cdc42 activity during cell polarity and cytokinesis in fission yeast. *Journal of cell science*. 132.
Hirota, K., K. Tanaka, K. Ohta, and M. Yamamoto. 2003. Gef1p and Scd1p, the Two GDP-GTP exchange factors for Cdc42p, form a ring structure that shrinks during cytokinesis in Schizosaccharomyces pombe. *Molecular biology of the cell*. 14:3617-3627.
Johnson, A.E., D. McCollum, and K.L. Gould. 2012. Polar opposites: Fine-tuning cytokinesis through SIN asymmetry. *Cytoskeleton*. 69:686-699.
Johnson, D.I. 1999. Cdc42: An essential Rho-type GTPase controlling eukaryotic cell polarity. *Microbiology and molecular biology reviews : MMBR*. 63:54-105.
Lamas, I., L. Merlini, A. Vjestica, V. Vincenzetti, and S.G. Martin. 2020a. Optogenetics reveals Cdc42 local activation by scaffold-mediated positive feedback and Ras GTPase. *PLoS biology*. 18:e3000600.

Lamas, I., N. Weber, and S.G. Martin. 2020b. Clustering-mediated activation of Cdc42 GTPase antagonized by GAPs in fission yeast. *bioRxiv*:2020.2006.2002.130336.
Martin-Cuadrado, A.B., E. Duenas, M. Sipiczki, C.R. Vazquez de Aldana, and F. del Rey. 2003. The endo-beta-1,3-glucanase eng1p is required for dissolution of the primary septum during cell separation in Schizosaccharomyces pombe. *Journal of cell science*. 116:1689-1698.
Martin-Cuadrado, A.B., J.L. Morrell, M. Konomi, H. An, C. Petit, M. Osumi, M. Balasubramanian, K.L. Gould, F. Del Rey, and C.R. de Aldana. 2005. Role of septins and the exocyst complex in the function of hydrolytic enzymes responsible for fission yeast cell separation. *Molecular biology of the cell*. 16:4867-4881.
McCusker, D., C. Denison, S. Anderson, T.A. Egelhofer, J.R. Yates, 3rd, S.P. Gygi, and D.R. Kellogg. 2007. Cdk1 coordinates cell-surface growth with the cell cycle. *Nature cell biology*. 9:506-515.
Merla, A., and D.I. Johnson. 2000. The Cdc42p GTPase is targeted to the site of cell division in the fission yeast Schizosaccharomyces pombe. *European journal of cell biology*. 79:469-477.
Mitchison, J.M., and P. Nurse. 1985. Growth in cell length in the fission yeast Schizosaccharomyces pombe. *Journal of cell science*. 75:357-376.
Moreno, S., A. Klar, and P. Nurse. 1991. Molecular genetic analysis of fission yeast Schizosaccharomyces pombe. *Methods in enzymology*. 194:795-823.
Murray, J.M., and D.I. Johnson. 2001. The Cdc42p GTPase and its regulators Nrf1p and Scd1p are involved in endocytic trafficking in the fission yeast Schizosaccharomyces pombe. *The Journal of biological chemistry*. 276:3004-3009.
Mutavchiev, D.R., M. Leda, and K.E. Sawin. 2016. Remodeling of the Fission Yeast Cdc42 Cell-Polarity Module via the Sty1 p38 Stress-Activated Protein Kinase Pathway. *Current biology : CB*. 26:2921-2928.
Nance, J., and J.A. Zallen. 2011. Elaborating polarity: PAR proteins and the cytoskeleton. *Development*. 138:799-809.
Nunez, I., M. Rodriguez Pino, D.J. Wiley, M.E. Das, C. Chen, T. Goshima, K. Kume, D. Hirata, T. Toda, and F. Verde. 2016. Spatial control of translation repression and polarized growth by conserved NDR kinase Orb6 and RNA-binding protein Sts5. *Elife*. 5.
Onwubiko, U.N., J. Rich-Robinson, R.A. Mustaf, and M.E. Das. 2020. Cdc42 promotes Bgs1 recruitment for septum synthesis and glucanase localization for cell separation during cytokinesis in fission yeast. *Small GTPases*:1-8.
Papadaki, P., V. Pizon, B. Onken, and E.C. Chang. 2002. Two ras pathways in fission yeast are differentially regulated by two ras guanine nucleotide exchange factors. *Molecular and cellular biology*. 22:4598-4606.
Perez, P., E. Portales, and B. Santos. 2015. Rho4 interaction with exocyst and septins regulates cell separation in fission yeast. *Microbiology*. 161:948-959.
Pino, M.R., I. Nuñez, C. Chen, M.E. Das, D.J. Wiley, G. D'Urso, P. Buchwald, D. Vavylonis, and F. Verde. 2020. Cdc42 GTPase Activating Proteins (GAPs) Maintain Generational Inheritance of Cell Polarity and Cell Shape in Fission Yeast. *bioRxiv*:2020.2006.2016.151308.

Pollard, T.D. 2010. Mechanics of cytokinesis in eukaryotes. *Current opinion in cell biology*. 22:50-56.
Pollard, T.D. 2014. The value of mechanistic biophysical information for systems-level understanding of complex biological processes such as cytokinesis. *Biophysical journal*. 107:2499-2507.
Ray, S., K. Kume, S. Gupta, W. Ge, M. Balasubramanian, D. Hirata, and D. McCollum. 2010. The mitosis-to-interphase transition is coordinated by cross talk between the SIN and MOR pathways in Schizosaccharomyces pombe. *The Journal of cell biology*. 190:793-805.
Revilla-Guarinos, M.T., R. Martin-Garcia, M.A. Villar-Tajadura, M. Estravis, P.M. Coll, and P. Perez. 2016. Rga6 is a Fission Yeast Rho GAP Involved in Cdc42 Regulation of Polarized Growth. *Molecular biology of the cell*.
Ridley, A.J. 2006. Rho GTPases and actin dynamics in membrane protrusions and vesicle trafficking. *Trends in cell biology*. 16:522-529.
Rincon, S., P.M. Coll, and P. Perez. 2007. Spatial regulation of Cdc42 during cytokinesis. *Cell cycle (Georgetown, Tex)*. 6:1687-1691.
Santos, B., A.B. Martin-Cuadrado, C.R. Vazquez de Aldana, F. del Rey, and P. Perez. 2005. Rho4 GTPase is involved in secretion of glucanases during fission yeast cytokinesis. *Eukaryotic cell*. 4:1639-1645.
Schmidt, S., M. Sohrmann, K. Hofmann, A. Woollard, and V. Simanis. 1997. The Spg1p GTPase is an essential, dosage-dependent inducer of septum formation in Schizosaccharomyces pombe. *Genes & development*. 11:1519-1534.
Schneider, C.A., W.S. Rasband, and K.W. Eliceiri. 2012. NIH Image to ImageJ: 25 years of image analysis. *Nat Methods*. 9:671-675.
Simanis, V. 2015. Pombe's thirteen - control of fission yeast cell division by the septation initiation network. *Journal of cell science*. 128:1465-1474.
Sipiczki, M. 2007. Splitting of the fission yeast septum. *FEMS Yeast Res*. 7:761-770.
Sopko, R., D. Huang, J.C. Smith, D. Figeys, and B.J. Andrews. 2007. Activation of the Cdc42p GTPase by cyclin-dependent protein kinases in budding yeast. *The EMBO journal*. 26:4487-4500.
Spector, I., N.R. Shochet, Y. Kashman, and A. Groweiss. 1983. Latrunculins: novel marine toxins that disrupt microfilament organization in cultured cells. *Science*. 219:493-495.
Swaffer, M.P., A.W. Jones, H.R. Flynn, A.P. Snijders, and P. Nurse. 2016. CDK Substrate Phosphorylation and Ordering the Cell Cycle. *Cell*. 167:1750-1761 e1716.
Takaine, M., O. Numata, and K. Nakano. 2009. Fission yeast IQGAP arranges actin filaments into the cytokinetic contractile ring. *The EMBO journal*. 28:3117-3131.
Tatebe, H., K. Nakano, R. Maximo, and K. Shiozaki. 2008. Pom1 DYRK regulates localization of the Rga4 GAP to ensure bipolar activation of Cdc42 in fission yeast. *Current biology : CB*. 18:322-330.
Tatebe, H., K. Shimada, S. Uzawa, S. Morigasaki, and K. Shiozaki. 2005. Wsh3/Tea4 is a novel cell-end factor essential for bipolar distribution of Tea1 and protects cell polarity under environmental stress in S. pombe. *Current biology : CB*. 15:1006-1015.

Tay, Y.D., M. Leda, A.B. Goryachev, and K.E. Sawin. 2018. Local and global Cdc42 guanine nucleotide exchange factors for fission yeast cell polarity are coordinated by microtubules and the Tea1-Tea4-Pom1 axis. *Journal of cell science*. 131.

Toda, T., H. Niwa, T. Nemoto, S. Dhut, M. Eddison, T. Matsusaka, M. Yanagida, and D. Hirata. 1996. The fission yeast sts5+ gene is required for maintenance of growth polarity and functionally interacts with protein kinase C and an osmosensing MAP-kinase pathway. *Journal of cell science*. 109 (Pt 9):2331-2342.

Tormos-Perez, M., L. Perez-Hidalgo, and S. Moreno. 2016. Fission Yeast Cell Cycle Synchronization Methods. *Methods Mol Biol*. 1369:293-308.

Wang, N., I.J. Lee, G. Rask, and J.Q. Wu. 2016. Roles of the TRAPP-II Complex and the Exocyst in Membrane Deposition during Fission Yeast Cytokinesis. *PLoS biology*. 14:e1002437.

Wang, N., M. Wang, Y.H. Zhu, T.W. Grosel, D. Sun, D.S. Kudryashov, and J.Q. Wu. 2015. The Rho-GEF Gef3 interacts with the septin complex and activates the GTPase Rho4 during fission yeast cytokinesis. *Molecular biology of the cell*. 26:238-255.

Wei, B., B.S. Hercyk, N. Mattson, A. Mohammadi, J. Rich, E. DeBruyne, M.M. Clark, and M. Das. 2016. Unique Spatiotemporal Activation Pattern of Cdc42 by Gef1 and Scd1 Promotes Different Events during Cytokinesis. *Molecular biology of the cell*. 27:1235-1245.

Win, T.Z., Y. Gachet, D.P. Mulvihill, K.M. May, and J.S. Hyams. 2001. Two type V myosins with non-overlapping functions in the fission yeast Schizosaccharomyces pombe: Myo52 is concerned with growth polarity and cytokinesis, Myo51 is a component of the cytokinetic actin ring. *Journal of cell science*. 114:69-79.

Figure Legends

Figure 1. Cytokinetic delay uncouples old end growth resumption from cell separation.
A) An asynchronous population of wild type cells was treated with 10μM Latrunculin A (LatA) for 30 minutes, and was then washed and allowed to recover. A subset of cells consistently show a phenotype wherein they form a septum as they resume growth and fail to undergo cell separation (asterisk next to original septum). These cells grow, and the septa formed in the next cell cycle separate normally (arrows). We call this the **P**ola**r** **E**longation **S**ans **S**eparation, or PrESS, phenotype. **B)** Time-lapse of two wild type cells after LatA washout, showing the PrESS phenotype. Growth resumed in the left cell at 60mins, and in the right cell at 85mins after washout (asterisks). **C)** PrESS cells resume growth significantly earlier in relation to septum closure than untreated cells (Student's t-test, $p < 0.0001$; $n \geq 10$ cells). **D)** *rng2-D5* cells were shifted to 36°C for 3 hours and then returned to permissive temperature at 25°C and allowed to grow. Asterisks denote growth initiation. Timestamps refer to time since completion of septum closure. Scale bars, 5μm.

Figure 2. The PrESS phenotype is cell-cycle-dependent.
A) Time-lapse imaging of cells undergoing LatA treatment and recovery. Vertical red bars denote cells undergoing a 30min 10μM LatA treatment. 0 time marks the timing of LatA washout. Rlc1-tdTomato and Sad1-mCherry mark the actomyosin ring and spindle pole bodies and indicate the cell cycle stage of the cells. Cells in G2 (i) or in G1/S (iii) at the time of LatA treatment do not show the PrESS phenotype during recovery. Cells in mitosis at the time of LatA treatment (ii) show the PrESS phenotype during recovery. The arrowhead marks the recovered actomyosin ring undergoing constriction. **B)** *cdc25-22* cells were synchronized by cell cycle block and release. During the indicated cell cycle stages occurring 0, 40, and 80 minutes after release, a fraction of cells was fixed and stained with phalloidin (magenta) and DAPI (cyan), to mark the actomyosin ring and nucleus respectively, while the rest were treated for 30 minutes with LatA and then washed. Cells recovering from LatA treatment in G2 or G1/S does not yield PrESS cells while those undergoing mitosis exclusively yield PrESS cells. Scale bars, 5μm.

Figure 3. Cdc42 is activated at the old ends prior to cell separation in PrESS cells.
A) Septum-digesting enzymes, Eng1-GFP and Agn1-GFP, in control cells show cortical distribution at the septum, effectuating a ring while in PrESS cells their localization appears as a disc all over the septum barrier. 3D-reconstructed membrane barriers are shown in the insets. **B)** Localization of the active Cdc42 marker CRIB-3xGFP in an untreated cell (top) and a PrESS cell (bottom). Asterisks denote growth onset. Arrowhead denotes loss of CRIB-3xGFP from the cell middle. Rlc1-tdTomato and Sad1-mCherry mark the actomyosin ring and spindle pole bodies and indicate the cell cycle stage of the cells. A single z-plane is shown for clarity and hence the sindle pole body is not visible in all the time frames. **C)** In untreated cells, Scd1-3xGFP, Scd2-GDP, and Myo52-tdTomato localize to the septum. When PrESS cells start to grow, all three disappear from the cell middle (arrowheads) and appear at the growing cell ends

(asterisks). Maximum projections of Myo52-tdTomato are shown, while single planes of Scd1-3xGFP and Scd2-GFP are shown. Scale bars, 5μm.

Figure 4. Loss of negative regulation of Cdc42 increases the incidence of the PrESS phenotype.
A, B) PrESS phenotype persists in mutants of Cdc42 activators *scd1Δ* and *gef1Δ*. *scd1Δ* does not show a significant change from wild type, while *gef1Δ* shows an increase ($p = 0.015$) (Ordinary 1-way ANOVA with Dunnett's multiple comparisons test). Asterisks denote PrESS cells. Repeated in triplicate, $n \geq 350$ cells per experiment. **C, D)** Loss of Cdc42 inactivator *rga4Δ* increases PrESS frequency during recovery from LatA treatment (Student's t-test, $p = 0.033$). Repeated in triplicate, $n \geq 350$ cells per experiment. Scale bars, 5μm.

Figure 5. Rga4 localization changes in a cell-cycle-dependent manner.
A) During G2, Rga4-GFP localizes to the cortex along the cell sides as distinct puncta. During mitosis (late and early anaphase) and septation (G1/S), Rga4-GFP at the cortex appears diffuse (parenthesis) with localization extending to the cell ends (asterisks). **B)** Time-lapse projection (10 sec intervals over 5 mins) of Rga4 localization at different cell cycle stages. Asterisk denotes enhanced tip localization in mitotic and G1/S cells. **C)** Rga4-GFP localization during G2 (asterisks) and early mitosis. Rlc1-tdTomato is a ring marker and here shows the formation of pre-ring nodes, and Sad1-mCherry is a spindle pole body marker used to show cell cycle stage. Arrows show Rga4-GFP localization to cell ends during early mitosis. **D)** Quantification of Rga4 localization to old ends through different cell cycle stages. e.a. = early anaphase; l.a. = late anaphase. (repeated in triplicate with $n \geq 7$ cells per experiment) **E)** Quantification of the Rga4-GFP localization pattern along the cell sides (increased co-efficient of variance = decreased homogeneity = increased punctate appearance) in wild type cells through different cell cycle stages. ($n \geq 10$ cells) **F)** *cdc2-as* mutant cells blocked in G2 upon 1NM-PP1 treatment show distinct Rga4-GFP puncta along the cell sides. After 1NM-PP1 washout, *cdc2-as* mutant enters mitosis and Rga4-GFP appears more diffuse along the cortex. Once in G1/S, Rga4-GFP again localizes as puncta. **G)** Quantification of the Rga4-GFP homogeneity along the sides in synchronized *cdc2-as* cells through different cell cycle stages. ($n \geq 14$ cells) Ordinary one-way ANOVA with Tukey's multiple comparisons. Scale bars, 5μm.

Figure 6. Deletion of *rga4* allows polarized growth in cells with constitutive MOR activity.
A) Cell expressing *nak1-mor2* (-thiamine) show cell lysis (red arrow) at the division site during cytokinesis in *rga4*$^+$ cells, while in *rga4Δ* mutants *nak1-mor2* expression leads to a PrESS-like phenotype in which cells fail separation and grow from the ends. **B)** Growth curve of *rga4*$^+$ or *rga4Δ* cells either expressing (-thiamine) or repressing (+thiamine) *nak1-mor2.* Optical density was measured every 15 minutes at 595nm for 2 days. (Ordinary one-way ANOVA with Tukey's multiple comparisons. **** = $p < 0.0001$; 5 experiments averaged for each genotype)

Figure 7. Model for growth resumption after cell division.
Rga4 localizes to the cell sides during G2. As the cells enter mitosis, Rga4 extends all the way to the cell ends. Upon activation of the anaphase-promoting complex, the MOR pathway is inactivated and Cdc42 activation and growth stop at the cell ends. After mitosis, MOR is activated and Rga4 localization is removed from the cell ends, which now resume growth. In PrESS cells, LatA treatment delays cytokinesis while mitosis continues to proceed, and the cell progresses to interphase. In these cells, Rga4 is removed from the cell ends before the completion of cytokinesis, resulting in Cdc42 activation and growth at cell ends at the expense of cytokinetic events at the cell middle. This suggests that growth resumption upon completion of cell division is independent of cytokinesis and dependent on cell-cycle cues.

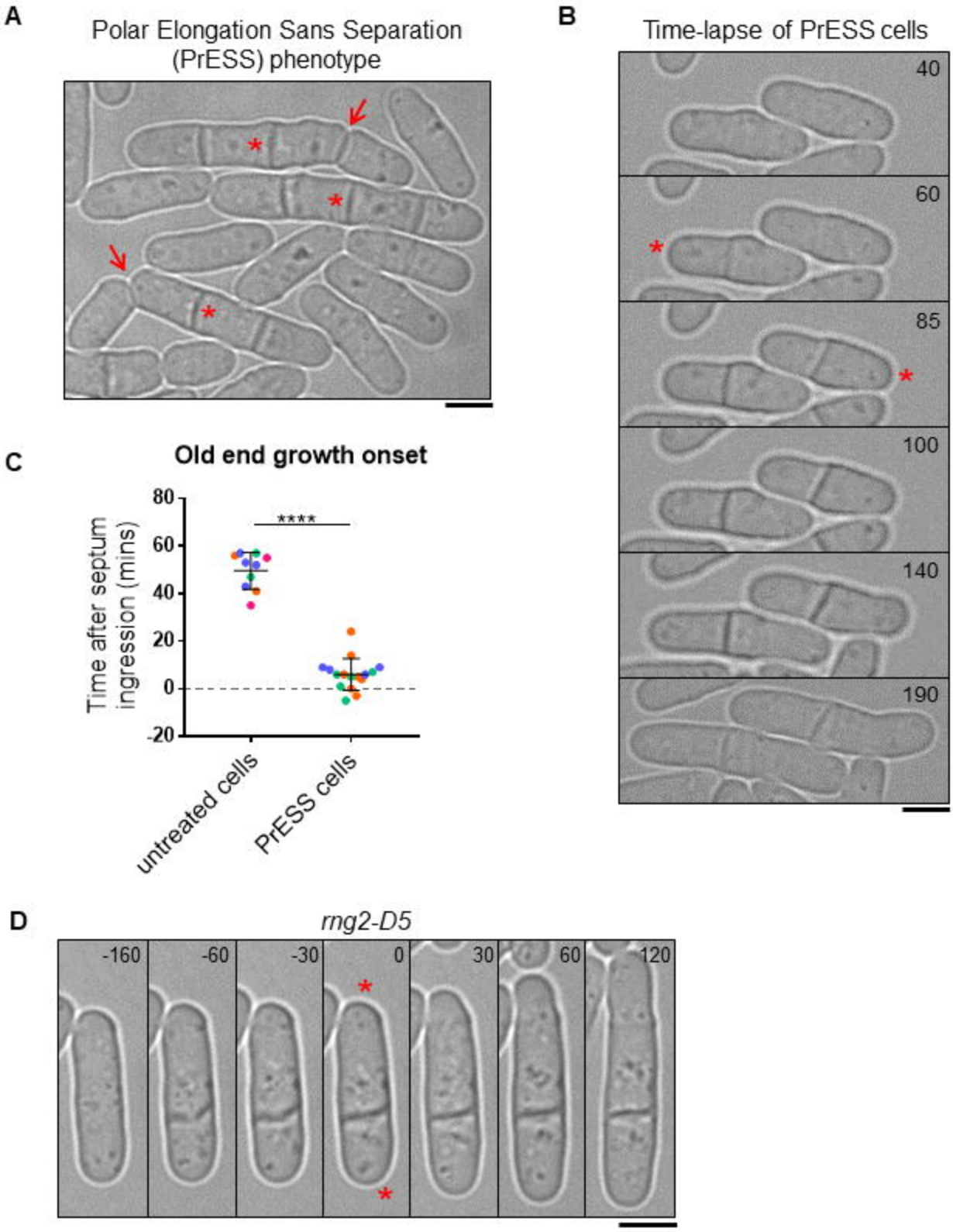
A
Polar Elongation Sans Separation (PrESS) phenotype
B
Time-lapse of PrESS cells
40
60
85
100
140
190
C
Old end growth onset
Time after septum ingression (mins)
80
60
40
20
0
-20
****
untreated cells
PrESS cells
D
rng2-D5
-160
-60
-30
0
30
60
120

Figure 1

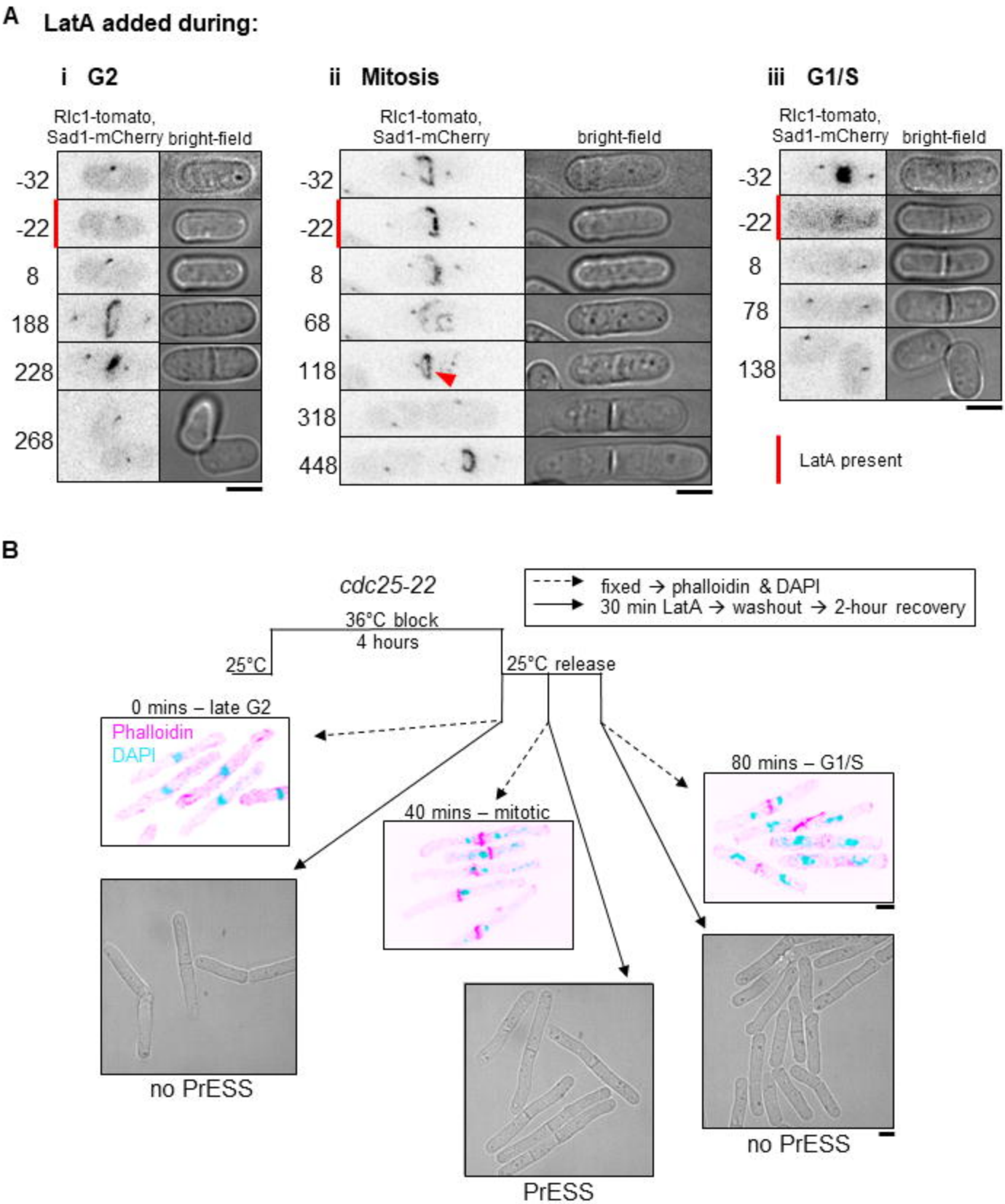
A
LatA added during:
i G2
ii Mitosis
iii G1/S
Rlc1-tomato, Sad1-mCherry
bright-field
-32
-22
8
188
228
268
68
118
318
448
78
138
LatA present
B
cdc25-22
fixed → phalloidin & DAPI
30 min LatA → washout → 2-hour recovery
36°C block
4 hours
25°C
25°C release
0 mins – late G2
Phalloidin
DAPI
40 mins – mitotic
80 mins – G1/S
no PrESS
PrESS
no PrESS

Figure 2

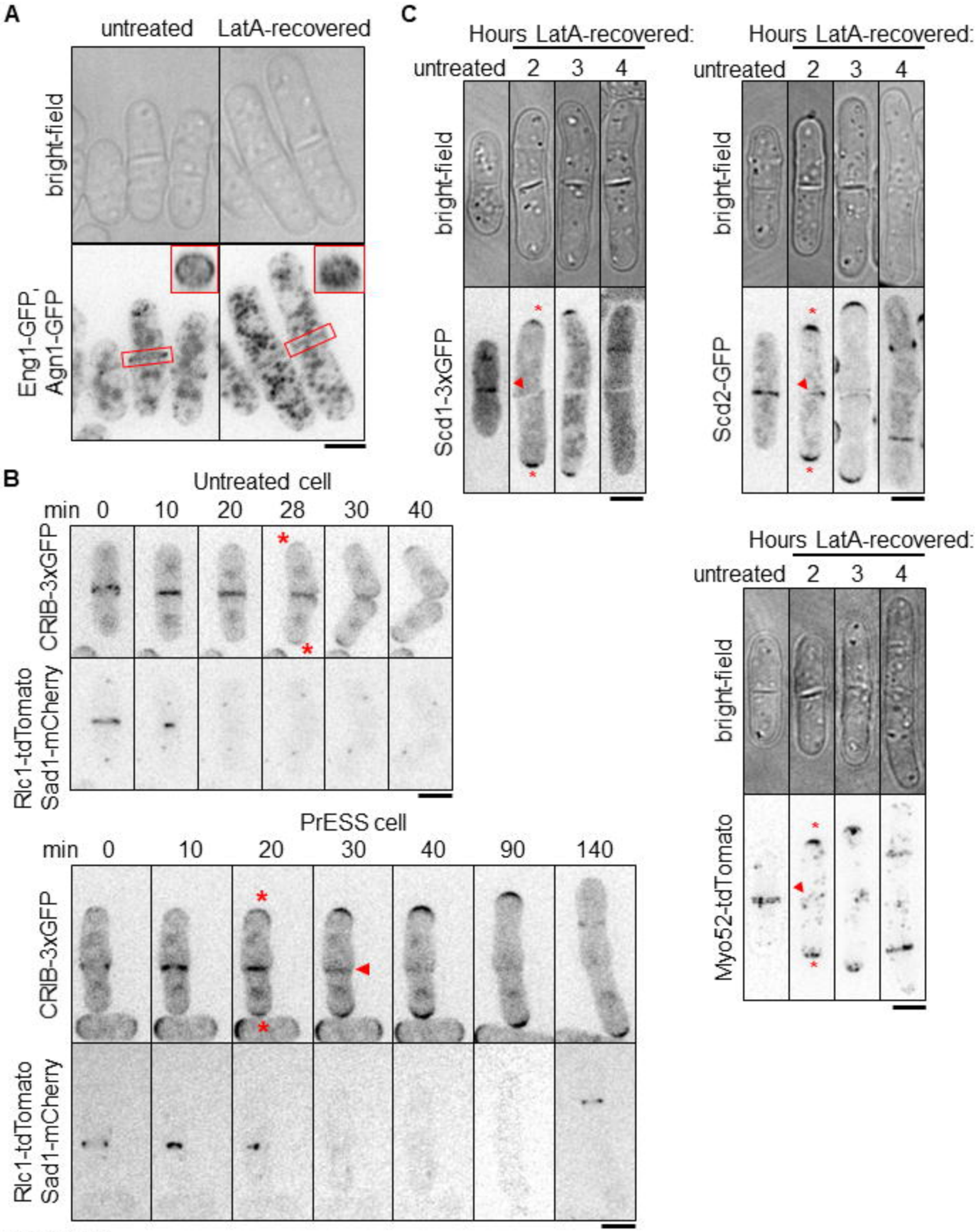
A
untreated
LatA-recovered
bright-field
Eng1-GFP,
Agn1-GFP
B
Untreated cell
min 0 10 20 28 30 40
CRIB-3xGFP
Rlc1-tdTomato
Sad1-mCherry
PrESS cell
min 0 10 20 30 40 90 140
CRIB-3xGFP
Rlc1-tdTomato
Sad1-mCherry
C
Hours LatA-recovered:
untreated 2 3 4
bright-field
Scd1-3xGFP
Hours LatA-recovered:
untreated 2 3 4
bright-field
Scd2-GFP
Hours LatA-recovered:
untreated 2 3 4
bright-field
Myo52-tdTomato

Figure 3

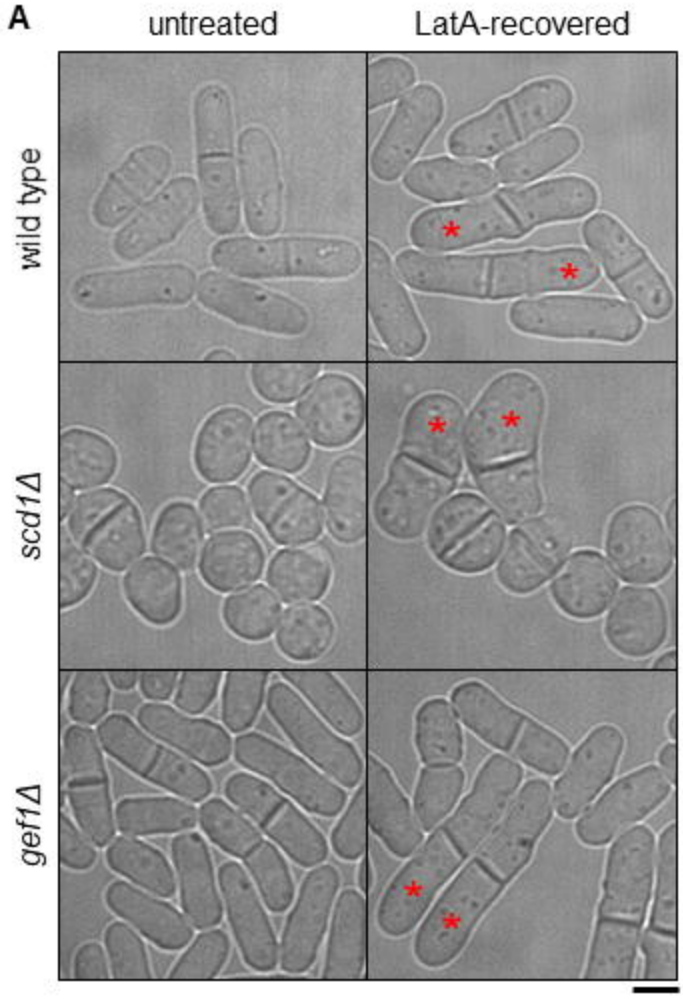

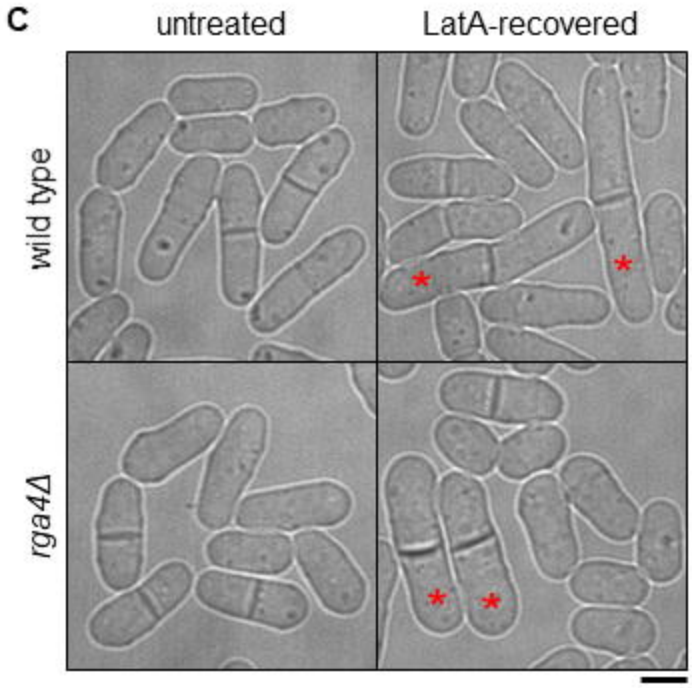

B

	Average peak PrESS cell frequency among LatA-recovered cells (%)
wild type	9.1 ± 0.8
scd1Δ	10.9 ± 2.0
gef1Δ	12.5 ± 0.4

D

	Average peak PrESS cell frequency among LatA-recovered cells (%)
wild type	9.2 ± 1.5
rga4Δ	12.9 ± 1.2

Figure 4

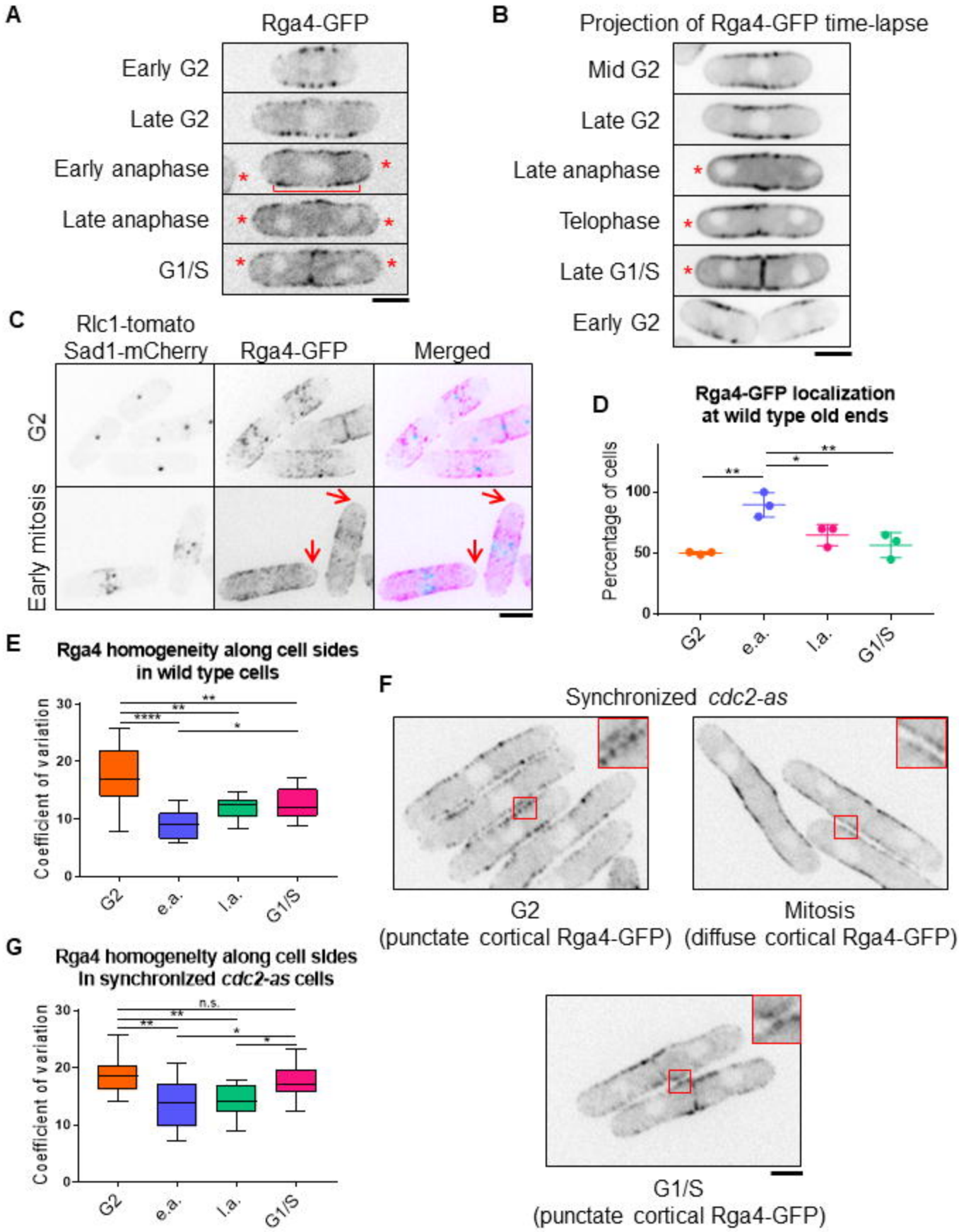
A
Rga4-GFP
Early G2
Late G2
Early anaphase
Late anaphase
G1/S
B
Projection of Rga4-GFP time-lapse
Mid G2
Late G2
Late anaphase
Telophase
Late G1/S
Early G2
C
Rlc1-tomato
Sad1-mCherry
Rga4-GFP
Merged
G2
Early mitosis
D
Rga4-GFP localization
at wild type old ends
Percentage of cells
100
50
0
G2
e.a.
l.a.
G1/S
E
Rga4 homogeneity along cell sides
in wild type cells
Coefficient of variation
30
20
10
0
G2
e.a.
l.a.
G1/S
F
Synchronized cdc2-as
G2
(punctate cortical Rga4-GFP)
Mitosis
(diffuse cortical Rga4-GFP)
G1/S
(punctate cortical Rga4-GFP)
G
Rga4 homogeneity along cell sides
in synchronized cdc2-as cells
Coefficient of variation
30
20
10
0
n.s.
G2
e.a.
l.a.
G1/S

Figure 5

A

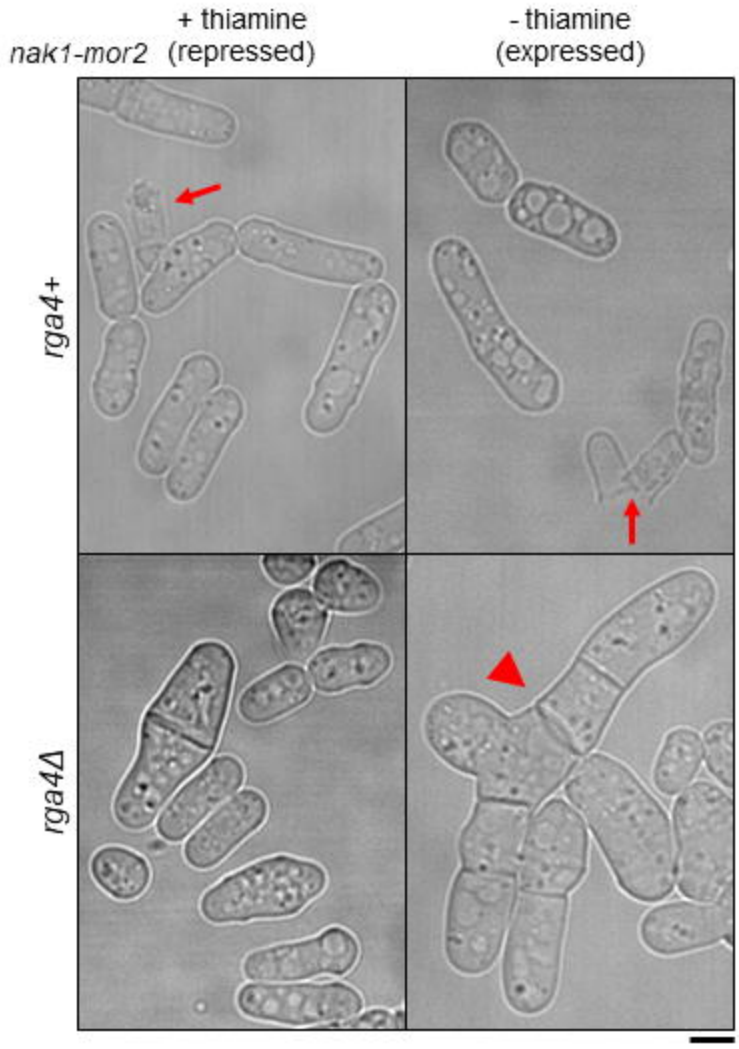
nak1-mor2
+ thiamine
(repressed)
- thiamine
(expressed)
rga4+
rga4Δ

B

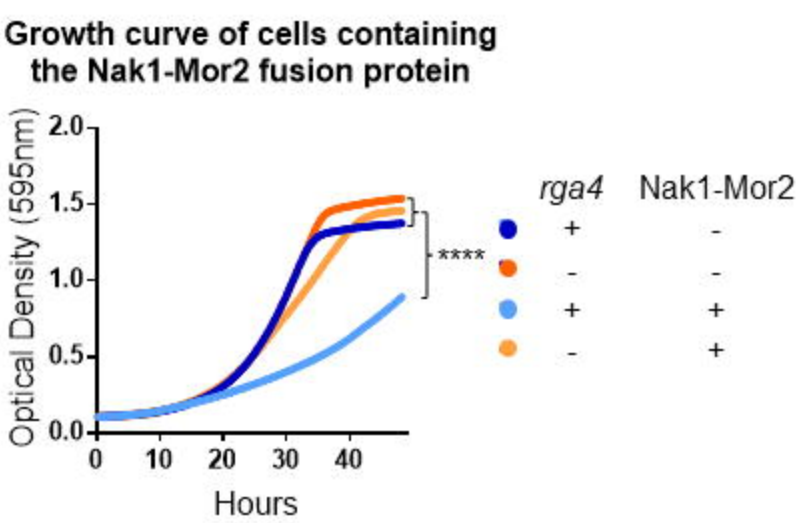
Growth curve of cells containing
the Nak1-Mor2 fusion protein
Optical Density (595nm)
2.0
1.5
1.0
0.5
0.0
0
10
20
30
40
Hours
****
rga4
Nak1-Mor2
+
-
-
-
+
+
-
+

Figure 6

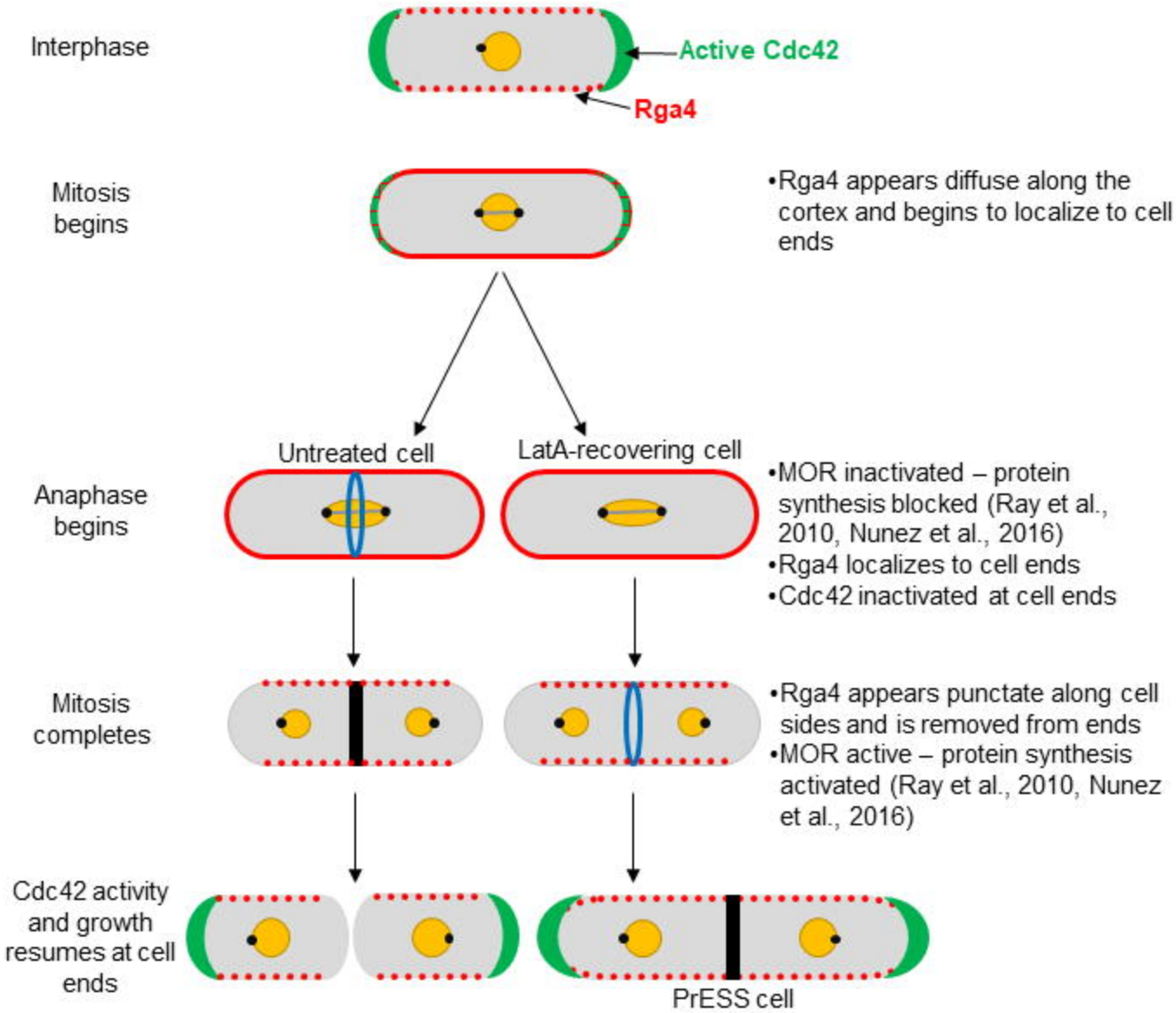
Interphase
Active Cdc42
Rga4
Mitosis begins
•Rga4 appears diffuse along the cortex and begins to localize to cell ends
Untreated cell
LatA-recovering cell
Anaphase begins
•MOR inactivated – protein synthesis blocked (Ray et al., 2010, Nunez et al., 2016)
•Rga4 localizes to cell ends
•Cdc42 inactivated at cell ends
Mitosis completes
•Rga4 appears punctate along cell sides and is removed from ends
•MOR active – protein synthesis activated (Ray et al., 2010, Nunez et al., 2016)
Cdc42 activity and growth resumes at cell ends
PrESS cell

Figure 7